Ice crystals growing from vapor in supercooled clouds between −2.5 and −22°C: testing current parameterisation methods using laboratory data

C. D. Westbrook *

Department of Meteorology, University of Reading, Berkshire, UK.

A. J. Heymsfield

NCAR, Boulder, Colorado, USA

* *Corresponding author address:* Chris Westbrook, Department of Meteorology, University of Reading, Earley Gate, PO Box 243, Reading, RG6 6BB.

E-mail: c.d.westbrook@reading.ac.uk

ABSTRACT

The physical and empirical relationships used by microphysics schemes to control the rate at which vapor is transferred to ice crystals growing in supercooled clouds are compared to laboratory data to evaluate the realism of various model formulations.

Ice crystal growth rates predicted from capacitance theory are compared to measurements from three independent laboratory studies. When the growth is diffusion-limited, the predicted growth rates are consistent with the measured values to within $\approx 20\%$ in 14 of the experiments analysed, over the temperature range -2.5 to $-22°$C. Only two experiments showed significant disagreement with theory (growth rate overestimated by $\approx$ 30–40% at -3.7 and $-10.6°$C).

Growth predictions using various ventilation factor parameterisations were also calculated and compared to supercooled wind tunnel data. It was found that neither of the standard parameterisations used for ventilation adequately described both needle and dendrite growth; however, by choosing habit-specific ventilation factors from previous numerical work it was possible to match the the experimental data in both regimes.

The relationships between crystal mass, capacitance, and fall velocity were investigated based on the laboratory data. It was found that for a given crystal size the capacitance was significantly overestimated by two of the microphysics schemes considered here, yet for a given crystal mass the growth rate was *underestimated* by those same schemes because of unrealistic mass-size assumptions. The fall speed for a given capacitance (controlling the residence time of a crystal in the supercooled layer relative to its effectiveness as a vapor sink, and the relative importance of ventilation effects) was found to be overpredicted by all the schemes in which fall-out is permitted, implying that the modelled crystals reside for

too short a time within the cloud layer, and that the parameterized ventilation effect is too strong.

1. Introduction

The occurrence of a thin layer of supercooled liquid water droplets at the top of cold clouds is a frequent occurrence in the atmosphere (Rauber and Tokay 1991). Simulation of such clouds in numerical models requires that the flux of vapor from liquid water droplets to the growing ice crystals is accurately predicted, along with the dynamical factors which promote condensation. These thin layer clouds often seem to maintain a small liquid water path in spite of the flux of vapour to ice crystals growing within the layer (Westbrook et al. 2010). Despite their low liquid water path, they are radiatively important (Hogan et al. 2003), and widespread globally (Hogan et al. 2004). General circulation models struggle to simulate them (Marsham et al. 2006), and although more sucess has been reported with cloud-resolving models (eg. Marsham et al. 2006; Smith et al. 2009) sensitivity of the simulated ice and liquid water contents to the assumed ice microphysics has also been reported by those same authors. The aim of this work is to explore some of the physical and empirical relationships which control the growth of ice (and hence the depletion of liquid) in model microphysics schemes, and compare these relationships to experimental measurements of ice crystals growing in laboratory supercooled clouds, in an attempt to validate and constrain some of the assumptions made in the parameterisation of this flux.

The datasets used are those reported by Mason (1953), Ryan et al. (1974, 1976) and Takahashi et al. (1991). These experiments have two features in common which limit the applicability of our analysis to natural clouds, and must be considered. First, the crystals were grown isothermally. This means that strictly the data analysed here can only be applied for growth times which are shorter than the time it takes the crystal to be transported (by

sedimentation or vertical air motion) to a level which is warmer or cooler by more than $\approx 1°C$. In weakly forced layer clouds this time may be several minutes; in the updraft of a cumulus cloud it may be a few tens of seconds. The second limitation is the method by which crystals were nucleated which in all cases was by very rapid cooling of a small region of air. This nucleation mechanism favours the formation of single crystals at temperatures as cold as $-39°C$ (eg Mason 1953), whilst droplets frozen by naturally occuring ice nuclei tend to form polycrystals below some critical temperature, dependent on the size of the droplet (Pitter and Pruppacher 1973). It is therefore important to consider whether these pristine single crystals are representative of the crystals grown in natural supercooled clouds over the temperature range considered here (-2.5 to $-22°C$).

A number of observational studies have examined the habits of crystals grown in thin supercooled clouds. Westbrook et al. (2010) used polarimetric radar observations to determine that pristine planar crystals were dominant in a persistent altocumulus layer 300m deep, cloud top $-15°C$, and in addition found that specular reflection from oriented planar crystals was present in the virga beneath 80% of supercooled layers between -12.5 and $-20°C$, based on 17 months of continuous measurements. Hogan et al. (2003) also reported pristine planar habits in aircraft obserations of a multilayered altocumulus cloud, cloud top $-15°C$, whilst in a second study where the cloud top was $-24°C$ the crystals appeared to be complex polycrystals. Carey et al. (2008) sampled several altocumulus cloud layers at temperatures between -12 and $-26°C$ and found pristine planar crystal habits near cloud top, with dendrites and aggregates commonly present lower down in the virga. Field et al. (2006) made in-situ and polarimetric radar observations of a supercooled stratocumulus cloud (top $-14°C$) and found that the ice virga was dominated by dendrites. Cooper and

Vali (1981) sampled crystals on oil coated glass slides in a decelerator whilst flying through thin supercooled cap clouds and observed small pristine plate crystals were dominant at the top in their first case study ($-21°$C), whilst hexagonal prisms near 1:1 aspect ratio were dominant in a second case (sampled at $-23°$C), although they also note the presence of a minority of planar polycrystals in that second case. aufm Kampe et al. (1951) grew crystals formed on natural ice nuclei in a (laboratory) supercooled fog and observed that planar polycrystals were dominant at $-22°$C. Collectively these studies suggest that single pristine crystals are common in thin mixed-phase clouds, and that the critical temperature for polycrystal formation lies somewhere in the range ≈ -20 to $-25°$C, depending on the details of the individual cloud. The data analysed in the present study covers the range -2.5 to $-22°$C, where it seems that single crystals are largely dominant, and we therefore expect that it should be reasonable to apply these results to many natural clouds. We note that in deep mixed-phase cloud layers (eg the complex mixed-phase stratus case studied by Fridlind et al. 2007) the situation may be much more complex: the effects of riming (Ono 1969), freezing of large drizzle drops (Korolev et al. 2006), and growth of accreted droplets (sometimes leading to polycrystal development, eg. Takahashi and Fukuta 1988) must also be considered – however this is beyond the scope of the present analysis.

Our analysis falls into two distinct parts. First, we test the basic growth equation used to model growth in numerical models. Houghton (1950) and Mason (1953) formulated the mass transfer from vapour to ice as:

$$\frac{\mathrm{d}m}{\mathrm{d}t} = 4\pi C \times \frac{(S-1)}{g} \times f \tag{1}$$

where m is the mass of the growing ice crystal at time t, $(S-1)$ is the supersaturation over

bulk ice, g is a function of temperature and pressure (Pruppacher and Klett 1997) and f is a ventilation factor. The capacitance C has units of length and acts as an effective radius for the non-spherical ice particle, controlling the flux of water molecules impinging on the crystal surface. The ventilation factor f characterises the forced convection produced as large ice crystals continuously fall into fresh supersaturated air. This enhances the growth rate relative to the growth of a stationary particle where the growth is limited purely by diffusion. For large enough particles $f \geq 1$ in Eq. (1). For small, slow-falling crystals in the first few minutes of growth, diffusion dominates and $f = 1$.

Methods to accurately calculate the capacitance of an ice particle with arbitrary geometry now exist (Westbrook et al. 2008, from now on W08). However it is clear that the underlying assumption of a uniform vapour density across the whole crystal surface (taken as the saturation value for bulk ice) is an approximation, and it is therefore important to compare theoretical growth rates with experimental measurements in order to determine whether the predicted growth rates are reliable, and in what range of conditions we can expect Eq. 1 to hold. Similarly, a variety of prescriptions have been developed for f (Hall and Pruppacher 1976; Ji and Wang 1999; Field et al. 2006), which have yet to be compared against experimental data.

The second part of our analysis focusses on the relationships which are needed to correctly integrate Eq. 1 forward in time (in particular the relationship between m and C) and the fall speed of the crystals relative to their growth rate (which acts to determine the net vapor flux during the crystal's residence within the liquid layer, as well as determining the influence of ventilation). These relationships are derived from the experimental data, and compared a number of parameterisations used in common bulk microphysics schemes.

The paper is organised as follows. Section 2 outlines the methodology for testing Eq. 1. In section 3, growth measurements in laboratory supercooled clouds (Mason 1953; Ryan et al. 1974, 1976) for growth times up to a few minutes are compared to calculations for pure diffusion-limited growth ($f = 1$). In section 4, data (Takahashi et al. 1991) from crystals grown for several minutes are analysed and compared to calculations using a variety of ventilation factor prescriptions. Finally, in section 5, we consider the empirical relationships between m, C and the fall speed v from various microphysical schemes and compare them to the relationships from the laboratory data.

2. Method for testing Eq. (1)

There are a number of studies which have measured the growth of ice crystals as a function of time (see, for example Pruppacher and Klett 1997). However, only a few have included all the necessary data to test Eq. (1) explicitly. To do this, time series of not only crystal mass, but also the crystal dimensions and details of the shape are required, along with knowledge of the environmental conditions. Using this data, Eq. (1) can be integrated and compared to the experimental time series of crystal mass $m(t)$. We prefer this approach to the alternative of attempting to differentiate the experimental data points (to estimate $\mathrm{d}m/\mathrm{d}t$) since the data are somewhat noisy and sparsely sampled in time.

Rather than integrating (1) from $t = 0$ (Fukuta 1969), we integrate forward from the first measured data point in the time series, and assess the accuracy of the predicted growth rate by comparing the integrated curve to the subsequent data points. Using this approach means that no assumptions on the (unobserved) initial shape/size evolution of the freshly

nucleated particle are necessary.

All of the experiments analysed here were carried out in supercooled liquid clouds, and hence the value of S is set equal to the saturation value for liquid water.

3. Short growth times: diffusion-limited growth

The earliest set of measurements which fit the criteria above were those made by Mason (1953). Crystals were grown by seeding a supercooled fog with dry ice in a $3.5 \times 2.5 \times 2.5$m chamber. Smooth, clear hexagonal plates and columns were found at temperatures $\geq -5°$C. The c- and a-axis dimensions of simple plate crystals grown at $-2.5°$C were measured at 20, 40, 80 and 120s after seeding; the crystal mass was estimated from these dimensions and the density of ice. Measurements of hexagonal column crystals (before the onset of hollow/needle growth) at $-5°$C at 40, 80, 120 and 160s were also made. Samples were taken by exposing slides for 10s periods, and a range of crystal sizes were observed on these samples: to ameliorate this problem Mason sub-sampled the largest 10% on each slide ($\approx$50 crystals), assuming these to be the last to be collected. The time series of the average mass of these crystals is plotted in Fig. 1. Also shown in this figure are the theoretical predictions obtained by integrating (1). Since the crystals involved were small ($< 65\mu$m), the growth is taken to be diffusion-limited, ie. $f = 1$. A linear fit was made to the crystal dimension measurements as a function of time, and the formula for hexagonal prisms in W08 was used to calculate the capacitance as a function of time. Comparing the theoretical curve with the experimental data, the predicted growth rate at $-2.5°$C is $\approx$ 10–20% higher than the measurements. Mason (1953) notes that there is 'considerable uncertainty' in measuring the

thickness of the plate crystals under the microscope, and this may be the source of this slight discrepancy. At -5°C there is excellent agreement, with the theoretical curve essentially indistinguishable from the experimental data. Mason himself calculated the growth over 40s periods by approximating his particles as spheroids and compared this calculation to the measured changes in mass, he drew a similar conclusion. These results suggest that Eq. 1 is successful to first order in this limited range of conditions. However, the unquantified errors in the measured masses emphasise the need for data from more carefully controlled experiments as a cross-check.

Ryan et al. (1974) formed a supercooled cloud in a 1.8m tall chamber and ice crystals were produced using the 'popping bubble' expansion technique. Time series of crystal mass (measured by melting the crystals) and their dimensions were obtained out to ≈ 3 minutes growth time at -5 (needles), -7 (hollow columns) and -9°C (solid columns). The mass measurements were digitised from the figures in their paper, and are shown in Fig. 2, whilst linear fits for the crystal dimensions are provided by Ryan et al. (1974). Additional data using the same apparatus were presented by Ryan et al. (1976) for -5 and -15°C. Because of the large number of data points at -5°C it was convenient to bin the data by growth time, and compute averages every 10s. Again the crystals were small ($< 300\mu$m) and we set $f = 1$ for our calculations. The formula of W08 was used to compute the capacitances: hollow columns and needles were taken to have the same capacitance as a solid column with the same dimensions (the data of McDonald 1963; Chiruta and Wang 2005 confirm the lack of sensitivity of C to these details). The capacitance of the stellar crystals growing at -15°C was calculated using the curve given in W08: the relative width of the branches was estimated from photographs in Ryan et al. (1976). Note that because the change in C

between different shaped planar crystals of a given size is rather small (see W08) we estimate the uncertainty associated with our interpolation of the crystal shape as a function of time from the photographs is unlikely to affect our $m(t)$ curves by $> 10\%$. We have assumed the growth is diffusion-limited: calculation of the ventilation effect for the largest crystals sampled here gave a maximum value of $f = 1.05$. Comparison between the measured and predicted curves are very encouraging: at -5 and -7°C there is excellent agreement, with the predicted growth rate accurate to within the experimental scatter. At -9°C good agreement is observed, albeit with a hint that the mass may be slightly overestimated at after 2 minutes of growth. At -15°C, agreement is again found to within the experimental scatter.

Note that in the discussion above we have implicitly assumed that the scatter in the experimental data may be considered a proxy for the experimental uncertainty. This is justified by Ryan et al. (1974)'s observation that the scatter in the observed crystal masses at a given time was significantly larger than the associated measurement errors, and this was deduced to be the result of variations in the time at which nucleation occurred (and hence the time for which the crystal had been growing). Based on Fig 2 this uncertainty is approximately $\pm$10s.

Additional measurements were made by Ryan et al. (1976) at temperatures down to -21°C: however only the results of their approximate power law fits at 50, 100 and 150s are recorded in their paper, rather than the measured $m(t)$ data themselves – because of this, we have not included these data in our analysis.

4. Longer growth times

The previous three studies only considered growth times up to 3 minutes because after this time even the rather small crystals produced had fallen out. To solve this problem Takahashi et al. (1991) suspended growing ice crystals individually in a supercooled wind tunnel, allowing growth from 3—30 minutes to be achieved, at temperatures between -3.8 and -22°C. Care must be taken with these long growth times however, since ventilation effects may be significant.

The experiments were isothermal and Figs. 3,4,5 show the comparison between the computed curves and Takahashi's measured growth data for each temperature (original data points provided by T. Takahashi, personal communication). There was some variation in temperature from run to run: the data here are filtered to remove points more than a degree from the target temperature. In each case the results for pure diffusion-limited growth are plotted as a solid black curve, and these predictions are appropriate to assessing the growth in the first minutes while the crystals are relatively small. Each data point refers to a single crystal grown at that temperature for that amount of time, which has then been removed from the supercooled tunnel, photographed and melted to obtain the particle mass. To calculate the capacitance, the fits for the dimensions of the crystals as a function of time from Takahashi et al. (1991) were used. The nucleation method was the same as Ryan et al. (1974), and we therefore anticipate a similar uncertainty in the growth time axis of $\pm$10s. In addition, each data point now corresponds to a separate experimental run. This introduces additional scatter in the data, since the temperature of each run is slightly different. Based on Fig.s 3-5, it appears that the latter is the primary source of experimental scatter, and

we proceed on the assumption that the experimental uncertainties are dominated by this scatter in the crystal masses, which is typically ± 20-30%.

To account for ventilation effects at longer growth times, equation (1) is usually multiplied by a ventilation factor $f \geq 1$. Various parameterisations of this effect are available in the literature: here we investigate the most common of these. Hall and Pruppacher (1976) introduced the prescription:

$$f = 1 + 0.14X_{L*}^2 \text{ if } X_{L*} < 1 \quad (2)$$

$$f = 0.86 + 0.28X_{L*} \text{ otherwise.} \quad (3)$$

where $X_{L*} = \mathrm{Sc}^{1/3}\mathrm{Re}_{L*}^{1/2}$. In the atmosphere the Schmidt number $Sc \approx 0.63$. In Hall and Pruppacher (1976)'s method the Reynolds number $\mathrm{Re}_{L*} = vL^*/\nu_k$ is defined based on the length scale L^*, the ratio of the total surface area of the particle to the perimeter of its projection normal to the flow. Here v is the fall speed of the crystal and ν_k is the kinematic viscosity of the air. The fall speeds of the crystals were inferred from the wind tunnel air speed required to keep the crystal stationary, and fits of $v(t)$ are given in Takahashi et al. (1991). The perimeter normal to the flow was determined from the crystal dimensions and knowledge of the preferred orientation of the hexagonal crystals as a function of aspect ratio (Westbrook 2010). For the branched crystal habits, Takahashi et al. (1991) estimated the perimeter and area of basal facets from photographs of the sampled crystals, and we use the fits from their paper. The dark grey dashed curves in figures 3,4,5 show the results when this ventilation factor is included. This ventilation correction will be referred to as HP.

The difficulty in estimating L^* from in-situ data, particularly for more complex shapes like dendrites, has led a number of researchers opting to simply substitute the maximum

dimension of the particle D in place of L^* in Eq. (3), (e.g. Field et al. 2006). The result of this approach is shown by the light grey dashed curves and will be referred to as HPD.

Finally, Ji and Wang (1999) have computed values of f from direct numerical simulations of the flow pattern around 3 idealised particles: a circular cylinder (intended as a proxy for columns/needles), a thin hexagonal plate, and a thin branched crystal. Where appropriate the numerical fits provided in Ji and Wang (1999) have been applied to compute the growth curves, and these are shown as solid light grey lines in Figs. 3,4. These calculations will be referred to as JW.

a. Planar crystals

Fig. 3 shows the results for planar crystals grown at −12.2 (thin hexagonal plates forming broad branches after 10 minutes of growth), −14.4 (thin stellar/dendritic crystals), −16.5 (broad branch planar crystals) and −18.2C (thick plates). Crystal capacitances were calculated from the formulae for hexagonal plates and branched planar crystals in W08, with transitions between the two estimated from the time series of photographs in Takahashi et al. (1991). At −14.4, −16.5 and −18.2°C the predicted growth in the diffusion-limited regime (where all of the numerical curves are the same) is in excellent agreement with the experimental data. After ≈ 10 minutes of growth, ventilation becomes significant: this is most apparent at −14.4 and −16.5°C where the growth was most rapid. In both cases the JW ventilation curves accurately predict the crystal mass to within experimental error. The HPD curves also work well for these particle types; however the HP curve was observed to substantially underpredict the measured crystal mass of the large stellar crystals at −14.4°C,

leading to the crystal mass being underestimated by a factor of 2 at 1500s, significantly larger than the apparent scatter at this range of growth times.. This is likely because the perimeter of these stellar and dendritic crystals is so long and tortuous, leading to a small value of L^* relative to the overall dimensions of the particle. This suggests L^* is not the correct length scale to use for these complex particle geometries.

The diffusion-limited growth curves at $-12.2°$C appear to slightly overestimate the early growth of the particles somewhat, by $\approx 20\%$. At longer growth times, the experimental data points lie around to the JW and HP ventilated curves.

b. Columns and needles

At $-5.3°$C hexagonal columns grew: these developed into a needle/sheath-like geometry as they grew larger than $\sim 100\mu$m. The capacitance of these particles was approximated by that of a hexagonal prism of the same overall dimensions: experimentation with more complex needle-like geometries using W08's method indicates that any numerical differences between the two are less than $\approx 10\%$. There is excellent agreement with the predicted growth and the measurements over two decades of crystal mass increase, as shown in Fig. 4. The growth appears to be largely diffusion-limited: the ventilation correction predicted by HP is relatively small, as is the JW ventilation factor for circular cylinders, and this is consistent with the experimental data. The HPD ventilation factor significantly overpredicts the growth rate at large sizes, leading to a crystal mass $\approx 40 - 50\%$ too high at 1500s. This discrepancy is significantly larger than the scatter in the data..

c. Isometric crystals

Fig. 5 shows the comparison between the measured and computed growth at −3.7, −8.6, −10.6, −20.1 and −22.0°C where the crystal growth was isometric, ie hexagonal prisms with an aspect ratio of approximately 1:1 were sampled. For these particles L^* and D are essentially the same, and so the HP and HPD correction factors are almost identical. Ji and Wang (1999) did not consider isometric crystal shapes, and so no JW curves are plotted in Fig. 5.

At −3.7°C the computed curves overestimate the growth relative to the laboratory-grown crystals by $\approx$ 30% on average. Computed ventilation effects are small, and the growth is essentially diffusion-limited over the 20 minutes. At −8.6°C on the other hand, close agreement between the measured and computed growth is observed throughout the first 10 minutes of growth. The last two data points suggest a rapid decrease in the growth rate after 10mins: it is not clear whether this is a measurement artefact. At −10.6°C, the computed growth is observed to be 30–40% faster than measured. At −20.1°C the predicted growth curves are consistent with the experimental data in the diffusion-limited regime (up to 450s); again, the last 3 data points seem to show a fall-off in the crystal growth rate. At −22.0°C good agreement is found with the experimental data following the computed growth curves to within experimental scatter.

5. Testing the empirical relationships controlling the flux of vapor from liquid to ice

The results above indicate that the sink of vapor to ice crystals growing in a supercooled cloud may be estimated with reasonable accuracy if the size, shape and fall speed of those crystals as a function of time are known a-priori. However, this information is often not available, and constraints based on parameterised relationships between the variables involved must be applied. In particular, operational numerical weather prediction and climate models are typically limited to one or two generic ice particle types (eg Wilson and Ballard 1999). Here we focus on three key relationships which determine how realistic the sink of vapor is in such models: the schemes tested here, along with the relevant parameters are listed in table 1.

First, we consider the capacitance of a crystal as a function of its linear dimensions: this is how ice growth is normally parameterised. Fig. 6 shows a normalised growth rate equal to the capacitance of a crystal (which has units of length) divided by its maximum span D in three dimensions[1]: the values are computed from Takahashi's measured crystal dimensions for the range of temperatures and growth times investigated in section 4. The isometric crystals have $C/D \approx 0.4$ with almost no variation over the growth history, while for crystals with more extended shapes (needles and planar crystals) the normalised growth rate is lower, decreasing from ≈ 0.35 at $D = 100\mu$m to as low as $C/D = 0.15$ for a 2mm needle. The grey line in Fig. 6 is $C/D = 0.5$, equal to the capacitance of a sphere with diameter D, as

[1]Note that this definition of D is not necessarily equal to that measured by two-dimensional imaging probes in-situ

used by Wilson and Ballard (1999). Fig. 6 indicates that this choice of parameter is too high, leading to an overestimate of the flux of vapor to the ice, by a factor of 2 or more in some cases. The choice of $C/D = 1/\pi$ by Rutledge and Hobbs (1983) is more realistic, lying roughly in the middle of the range of experimental values. This value was also applied by Hong et al. (2004) for use in the Weather Research and Forecasting (WRF) model. The scheme of Thompson et al. (2008) (also commonly used in WRF) parameterises a value of $C/D = 0.5$ for cloud ice (particles with $D < 200\mu$m) and a temperature dependent value for their snow category ($D > 200\mu$m) varying linearly from 0.5 at -30°C to 0.3 at -15°C, and constant above/below. The range of predicted values for snow corresponding to the temperature range considered in this paper ($T \geq -22$°C, $C/D = 0.4$–0.3) is indicated on Fig 6 as a dark grey shaded region. The value of 0.5 for cloud ice is an overestimate at all temperatures as before, whereas the range of values predicted for snow is more realistic, albeit overestimating C for needles by up to a factor of 2.

The second relationship we consider is that between the capacitance of a crystal and its mass. This relationship is crucial to integrating Eq. (1) for cases where the growth is diffusion-limited: for a given particle mass it controls the rate at which that mass will increase. Fig. 7 shows this relationship for the Takahashi et al. (1991) data set, with capacitances computed as described in section 4. Again, there is a factor of 2 variability in the data from temperature to temperature, with the most efficient growth occurring at -14.4°C. Note that in most microphysics parameterisations this $C(m)$ relationship, although important, is usually implicit, and made up of two components: an $m(D)$ relationship and a $C(D)$ relationship. Wilson and Ballard (1999) use Cox (1988)'s mass-size relationship, and this together with the $C/D = 0.5$ assumption leads to the solid grey curve in Fig. 7. In spite

of the fact that the spherical assumption yields a growth rate for a given particle size which is higher than any of the Takahashi data, the relatively dense particles predicted by the Cox relation means that the predicted growth rate for a given particle *mass* is actually lower than any of the data. This implies that the predicted crystal mass of a particle at a given time since nucleation is actually too low using this scheme. Altering $m(D)$ to follow the common Brown and Francis (1995) relationship (referred to from now on as the modified W&B scheme) leads to faster growth for a particle of given mass and a more realistic capacitance, albeit still lying along the lower edge of the spread of data. The assumptions used in Rutledge and Hobbs (1983) give a significantly higher growth rate, lying on the upper edge of the data for cloud ice ($D < 500\mu$m). For larger particles classified as snow, the growth rate is reduced, but still lying within the range of Takahashi's data. The Hong et al. (2004) scheme predicts a reasonably realistic $C - m$ relationship, with the rapid growth at -5.3 and -16.5°C being most accurately captured. Note that we are using Hong et al. (2004)'s 'snow' category since their model immediately converts all cloud ice to snow in the temperature range considered here. The Thompson et al. (2008) scheme (shaded region marked T08) predicts a $C - m$ relationship near the middle of the Takahashi data for cloud ice, but predicts much slower growth for snow, and as for Wilson and Ballard (1999) this is most likely because of the application of the Cox (1988) $m(D)$ relationship.

An early parameterisation of vapor growth in supercooled clouds was provided by Koenig (1971), and the results from this study are still applied to modeling of the Bergeron Findeison process in a number of contemporary microphysics schemes (eg Zeng et al. 2009). This parameterisation takes the form $\frac{\mathrm{dm}}{\mathrm{d}t} = a_1 m^{a_2}$, where a_1 and a_2 are constants determined as a

function of temperature[2], and ventilation effects are included. It is of course possible to use Eq. 1 to recast the parameterised growth rates in terms of the product $C \times f$, and Fig 9c shows the ratio of this product as determined by Koenig's relationships relative to the values we have derived from Takahashi's data (for ventilation we have used the JW values where appropriate, and neglected ventilation for the other, relatively small, crystals). While the predicted values are broadly realistic in magnitude, the errors at individual temperatures can be as much as a factor of 2. At the time at which Koenig devised his scheme there was almost no experimental data to guide him: Fig. 9 strongly suggests that a revision of his a_1, a_2 parameters as a function of temperature is warranted if this scheme continues to be applied. In this vein we have fitted power laws of the form $Cf = b_1 m^{a_2}$ to the values derived from Takahashi's data - these are given in table 2. Also given are new values of a_1 which can be substituted into Koenig's formula. Linking Cf to m may be preferred to Koenig's approach, since the values of b_1 are independent of pressure, whilst the values of a_1 given in table 2 are computed explicitly for 1000hPa.

Finally, the relationship between the crystal capacitance and its fall speed is investigated. This relationship is significant for the depletion of the liquid water in supercooled layer clouds for two reasons: (i) because it controls the relative magnitude of the flux of water vapor to ice versus the residence time of that ice (*i.e.* the residence time of the vapor sink) in the supercooled layer; (ii) because it controls the relative influence of ventilation factor f in equation 1. Fig. 9d shows $v(C)$ from Takahashi et al. (1991)'s fits. Again, in model schemes this relationship is implicit, usually $C(D)$, $v(D)$ relationships are explicitly parameterised,

[2]Note that there appears to be a typographical error in Koenig's table 4: at -14°C we have taken $a_1 = 0.1725 \times 10^{-4}$ rather than the (very unrealistic) tabulated value of $a_1 = 0.1725 \times 10^{-6}$.

leading to an implicit $v(C)$. Fig 9d shows the Wilson and Ballard (1999) parameterisation where the crystals are modelled to fall out appreciably faster than occurs in Takahashi's experiments. The Thompson et al. (2008) scheme leads to fall speeds slightly faster than Wilson and Ballard (1999). In Rutledge and Hobbs (1983) the 'cloud ice' does not sediment until converted to snow - hence the removal of small ice is underestimated; by contrast the predicted snow terminal velocities are significantly higher than measured. The Hong et al. (2004) scheme is found to give results close to the fall speeds of the small isometric crystals, but strongly overestimates the fall out of larger particles with a capacitance $> 100\mu$m. The results in Fig 9d suggest that parameterised fall speeds are generally overestimated in the models considered here, and hence the simulated total sink of vapor from the droplets to each crystal will be too low.

To investigate the second point, the lower panel of figure 7b shows the product of $C \times f$ as function of crystal mass - this is the complete product which is integrated in Eq. 1 to obtain $m(t)$. Wilson and Ballard (1999), Rutledge and Hobbs (1983) and Hong et al. (2004) all use Thorpe and Mason (1966)'s ventilation factor $f = 0.65 + 0.44X_{L*}^{1/2}$ for snow, except that the maximum dimension D is substituted for L^*, as Field et al. (2006) did for Hall and Pruppacher (1976)'s formula[3]. Thompson et al. (2008) uses the HPD formula for f. The resulting curves for the Wilson and Ballard (1999), modified W&B scheme and Thompson et al. (2008) are improved relative to the pure *mass-capacitance* plot in figure 7a. This improved agreement is essentially the result of two compensating errors - a $C(m)$ curve which is too low, and a $v(C)$ curve (and hence ventilation effect) which is too high.

[3]Thorpe and Mason (1966) was not evaluated in section 4, because their fit applies only over a limited region of X_{L^*}. Most models however simply extrapolate this fit to all sizes

The Rutledge and Hobbs (1983) curves for snow now lie closer to the data for rapid growth of needles and dendrites, rather than the isometric crystals. The relatively realistic $C(m)$ curve predicted by Hong et al. (2004) however now overestimates the growth rate for particles larger than 1μg, because of the rapid fall speeds which it predicts.

We note that the above analysis relates to the relationships needed to evolve the mass of a single crystal forward in time. In practice, bulk schemes integrate this mass increment over a complete size spectrum, which is also parameterised (usually based on ice water content and temperature). This strongly affects how the growth parameters discussed here add up to determine the rate of change of ice water content in a grid box. However, if the basic relations considered above are not realistic, there is no reason to suppose that the net effect of a whole spectrum of ice crystals will be any more so, unless compensating errors are present in the size spectrum description. This issue is important, but beyond the scope of the present analysis.

6. Discussion

We have compared the predicted growth rates using capacitance theory to experimental growth rates measured in laboratory supercooled clouds from three different experimental set-ups, at temperatures between -2.5 and -22°C. In all three experiments, the growth rates predicted using Eq. (1) were found to be realistic, and in most cases fell within the scatter present in the experimental data for the diffusion-limited regime. This is an important result for modellers simulating the water budget in mixed-phase layer clouds (Smith et al. 2009) and for observers seeking to estimate these budget terms from in-situ size spectra. The

largest discrepancies were found at -3.7, -10.6°C (Takahashi et al. 1991) where the growth rate appeared to be overestimated by as much as 40%: whether this represents a physical feature of the growth at these temperatures or is simply experimental artefact requires further investigation. Overall, the comparisons in sections 3 and 4 give us confidence that the growth rate may be predicted with reasonable accuracy using the capacitance method.

Of the three sets of ventilation parameterisations, JW was consistent with the experimental data in all cases: note however that this parameterisation is different for different crystal habits, and no equation for isometric particles is available. The HP method was found to give realistic results for relatively simple hexagonal shapes, but predicted almost no ventilation for dendrites leading to disagreement with the experimental data. The HPD approach on the other hand worked well for planar and isometric crystals, but strongly overestimated the ventilation effect for needles.

The biggest uncertainty in predicting the vapour growth of newly-formed ice crystals in supercooled clouds appears to be determining the relationship between a crystal's mass and its growth rate (ie. the product of capacitance $\times$ ventilation factor). This uncertainty feeds directly into the integration of Eq. (1) to obtain $m(t)$ and the experimental data here indicate a factor of ~ 2 variation of this relationship with temperature, posing a challenge for modellers. The adaptive growth model of Chen and Lamb (1994) may be one solution. Another approach is to parameterise a variable relationship as a function of temperature based on the data here (see table 2): however the growth history of crystals in the atmosphere is rarely isothermal at 1000hPa, and is modulated by convective air motions and crystal fall trajectories. It could be that this non-isothermal growth history may wash out some of the sensitivity exhibited in the experiments. This is an unknown (but potentially important)

factor and simulation of such growth in the laboratory remains a major challenge. In spite of this, the analysis in section 5 are a useful tool to assess to first order whether a microphysical scheme is predicting growth rates and fall speeds which lie within a realistic range. This following curves approximately describe the upper and lower bounds of the experimental data respectively: $C \times f\ [\mu\mathrm{m}] = 3.5 \times m\ [\mathrm{ng}]^{0.6}$ and $Cf = 8m^{0.3}$: these bounds may be compared with the relationships in a given model. The important caveat is that the cloud is dominated by single pristine crystals, as discussed in section 1: the range of temperature, liquid water path and drop size distribution over which this is valid is not fully understood at present, and more observational work sampling is needed to quantify this..

We have found that the parameterisation of Koenig (1971) does not accurately predict the temperature dependent growth rate in isothermal conditions, and have suggested revised parameters which could be applied to correctly capture isothermal growth.

The fall speed of ice crystals growing at a given rate is also poorly predicted in the microphysics schemes considered here, leading to an unrealistically short residence time in the cloud layer, and an unrealistically high ventilation factor for larger crystals.

Although our article has focussed primarily on thin layer clouds, the results may also be useful to some degree in convective clouds. Figure 10 shows an example of crystals collected in a narrow convective cell (top $-12°$C, peak updraft 1m/s: see Crosier et al. 2011 for full details): large concentrations ($\approx 20\mathrm{l}^{-1}$) of pristine sheaths and needles produced by the Hallett-Mossop rime-splintering process (Pruppacher and Klett 1997) were observed in this cloud near the $-5°$C level. Importantly, our result show that the vapor growth of these needles may be adequately modeled by simple capacitance theory. More generally, our results should also apply to the early growth of ice formed on natural nuclei, before

the onset of riming. Ono (1969) found that riming was not observed until crystals were at least a critical size: this critical value was $D = 300$–400μm for planar crystals, whilst for columnar types the critical *diameter* was found to be 50–90μm (in terms of column *length* the range of critical values is much wider: Ono observed rimed columns as small as 100μm, whilst sheaths/needles as large as 600μm were observed to be completely pristine, as also seen in figure 10). These critical values have been confirmed by Kajikawa (1974) and Baker and Lawson (2006).

The applicability of the analysis in section 5 is perhaps more limited for convective clouds since the approximation of isothermal growth is valid only over a short time period, and the details of $C(m)$, $v(C)$ at longer growth times will likely vary from case to case depending on the vertical air motion.

Finally, we remark that the validity of Eq. (1) at temperatures colder than -22°C has yet to be established, and we should be wary of extrapolation of the present analysis to colder temperatures. Some laboratory measurements in cold conditions have suggested that the assumption of a crystal surface which is saturated with respect to bulk ice can break down (Magee et al. 2006; Bailey and Hallett 2004). In addition the growth of more complex polycrystalline forms leads to new $C - D$, $m - C$ and $v - C$ relationships. Likewise, our analysis is limited to growth in water-saturated clouds: new data would be valuable to test computed growth rates at lower supersaturations over the same temperature range. More laboratory and observational data is urgently needed to determine these relationships and the range of applicability of (or magnitude of deviations from) Eq. (1) as a function of temperature, supersaturation and particle size.

Acknowledgments.

CDW was supported by the Natural Environment Research Council; AJH was funded by the National Science Foundation. We would like to thank T. Takahashi for supplying the original data used in section 4. Detailed reviews from Dr. Ann Fridlind and 2 anonymous reviewers greatly improved the quality of this manuscript.

REFERENCES

aufm Kampe HJ, Weickmann HK and Kelly JJ 1951. The influence of temperature on the shape of ice crystals growing at water saturation. *J. Met.* **8**: 168–174

Bailey M and Hallett J 2004. Growth rates and habits of ice crystals between −20 and −70°C. *J. Atmos. Sci.* **61**: 514–544

Baker BA and Lawson RP 2006. In situ observations of the microphysical properties of wave, cirrus, and anvil clouds. Part I: Wave clouds. *J. Atmos. Sci.* **63**: 3160–3185

Brown PRA and Francis PN 1995. Improved measurements of the ice water content of cirrus using an evaporative technique. *J. Atmos. & Ocean. Tech.* **10**: 579–590

Carey LD, Niu J, Yang P, Kankiewicz JA, Larson VE, Vonder Haar TH, 2008. The Vertical Profile of Liquid and Ice Water Content in Midlatitude Mixed-Phase Altocumulus Clouds. *J. Appl. Meteor. Climatol.* **47**: 2487–2495

Chen J and Lamb D 1994. The theoretical basis for the parameterisation of ice crystal habits: growth by vapor deposition. *J. Atmos. Sci.* **51**: 1206–1221

Chiruta M and Wang PK 2005. The capacitance of solid and hollow hexagonal ice columns. *Geophys. Res. Lett.* **32**: L05803

Cooper WA and Vali G 1981. The origin of ice in mountain cap clouds. *J. Atmos. Sci.* **38**: 1244–1259

Cox GP 1988. Modelling precipitation in frontal rainbands. *Q. J. R. Meteorol. Soc.* **114**: 115–127

Crosier J *et al.* 2011. Observations of ice multiplication in a weakly convective cell embedded in supercooled mid-level stratus. *Atmos. Chem. Phys.* **11**: 257–273

Field P, Heymsfield AJ, Bansemer A and Twohey CH 2006. Determination of the combined ventilation factor and capacitance for ice crystal aggregates from airborne observations in a tropical anvil cloud. *J. Atmos. Sci* **65**: 376–391

Fridlind AM, Ackerman A, McFarquhar G, Zhang G, Poellot MR, DeMott PJ, Prenni AJ and Heymsfield AJ 2007. Ice properties of single-layer stratocumulus during the mixed-phase arctic cloud experiment: 2. model results. *J. Geophys. Res.* **112**: D24202

Fukuta N 1969. Experimental studies on the growth of small ice crystals. *J. Atmos. Sci.* **26**: 522–531

Hall W and Wang PK 1976. The survival of ice particles falling from cirrus clouds in sub-saturated air. *J. Atmos. Sci.* **57**: 916–938

Hogan RJ, Francis PN, Flentje H, Illingworth AJ 2003. Characteristics of mixed-phase clouds: Part I: Lidar, radar and aircraft observations from CLARE'98 *Quart. J. Roy. Meteorol. Soc.* **129**: 2089–2116

Hogan RJ, Francis PN, Flentje H, Illingworth AJ 2003. Estimating the global distribution of supercooled liquid water clouds using spaceborne lidar *Geophys Res. Lett.* **32**: L05106

Hong SY, Dudhia J and Chen SH 2004. A revised approach to ice microphysical processes for the bulk parameterisation of clouds and precipitation *Mon. Wea. Rev.* **132**: 103–120

Houghton HG 1950. A preliminary quantitative analysis of precipitation mechanisms. *J. Met.* **7**: 363–369

Ji W and Wang PK 1999. Ventilation Coefficients for Falling Ice Crystals in the Atmosphere at Low and Intermediate Reynolds Numbers. *J. Atmos. Sci.* **56**: 829–836

Kajikawa M 1974. On the collection efficiency of snow crystals for cloud droplets. *J. Meteorol. Soc. Jap.* **52**: 328–356

Koenig LR 1971. Numerical modeling of ice deposition. *J. Atmos. Sci.* **28**: 226–237

Korolev AV, Bailey MP, Hallett J and Isaac GA 2004. Laboratory and In Situ Observation of Deposition Growth of Frozen Drops. *J. Appl. Meteorol.* **43**: 612–622

Lawson RP et al. 2006. The 2D-S (stereo) probe: design and preliminary tests of a new airborne, high-speed, high-resolution, particle imaging probe. *J. Atmos. & Ocean. Tech.* **23**: 1462–1477

Magee N, Moyle AM and Lamb D 2006. Experimental determination of the deposition coefficient of small cirrus-like ice crystals near −50°C. *Geophys. Res. Lett.* **33**: L17813

Marsham JH, Dobbie S and Hogan RJ 2006. Evaluation of a large-eddy model simulation of a mixed-phase altocumulus cloud using microwave radiometer, lidar and Doppler radar data. *Q. J. R. Meteorol. Soc.* **132**: 1693–1715

Mason BJ 1953. The growth of ice crystals in a supercooled water cloud. *Q. J. R. Meteorol. Soc.* **79**: 104–111

McDonald JE 1963. The use of the electrostatic analogy in studies of ice crystal growth. *Z. Angew. Math. Phys.* **14**: 610–619

Ono A 1969. The shape and riming properties of ice crystals in natural clouds. *J. Atmos. Sci.* **26**: 138–147

Pitter RL and Pruppacher HP 1973. A wind tunnel investigation of freezing of small water drops falling at terminal velocity in air. *Q. J. R. Meteorol. Soc.* **99**: 540–550

Pruppacher HR and Klett JD 1997. *Microphysics of clouds and precipitation.* second edition, Kluwer, London 954pp.

Rauber RM, Tokay A 1991. An explanation for the existence of supercooled liquid water at the top of cold clouds. *J. Atmos. Sci.* **48** 1005-1023.

Rutledge SA and Hobbs PV 1983. The mesoscale and microscale structure and organisation of clouds and precipitation in midlatitude cyclones. VIII: a model for the "seeder-feeder" process in warm-frontal rainbands. *J. Atmos. Sci.* **40**: 1185–1206

Ryan BF, Wishart ER and Holroyd EW. The densities and growth rates of ice crystals between -5 and -9°C. *J. Atmos. Sci.* **31**: 2136–2141

Ryan BF, Wishart ER and Shaw DE 1976. The growth rates and densities of ice crystals between -3 and -21°C. *J. Atmos. Sci.* **33**: 842–850

Smith AJ, Larson VE, Niu J, Kankiewicz JA and Carey LD 2009. Processes that generate and deplete liquid water and snow in thin midlevel mixed-phase clouds. *J. Geophys. Res.* **114**: D12203

Takahashi T and Fukuta N 1988. Supercooled cloud tunnel studies on the growth of snow crystals between -4 and -20°C. *J. Meteorol. Soc. Jap.* **66**: 841–855

Takahashi T, Endoh T and Wakahama G 1991. vapor diffusional growth of free-falling snow crystals between -3 and -23°C. *J. Meteorol. Soc. Jap.* **69**: 15–30

Thompson G, Field PR, Rasmussen RM and Hall WD 2008. Explicit forecasts of winter precipitation using an improved bulk microphysics scheme. Part II: implementation of a new snow parameterization. *Mon. Wea. Rev.* **136**: 5095–5115

Thorpe AD and Mason BJ 1966. The evaporation of ice spheres, and ice crystals. *Brit. J. Appl. Phys.* **17**: 541–551

Westbrook CD, Hogan RJ and Illingworth AJ 2008. The capacitance of pristine ice crystals and aggregate snowflakes. *J. Atmos. Sci.* **65**: 206–219

Westbrook CD 2010. Origin of the Parry arc. *Q. J. R. Meteorol. Soc.* **137** 538-543

Westbrook CD, Illingworth AJ, O'Connor EJ and Hogan RJ 2010. Doppler lidar measurements of oriented planar ice crystals falling from supercooled and glaciated cloud layers. *Q. J. R. Meteorol. Soc.* **136**: 260–276

Wilson DA and Ballard SP 1999. A microphysically based precipitation scheme for the UK Meteorological Office Unified Model. *Q. J. R. Meteorol. Soc.* **125**: 1607–1636

Zeng X, Tao W-K, Zhang M, Hou AY, Xie S, Lang S, Li X, O'C. Starr, D, Li X, Simpson J 2009. An Indirect Effect of Ice Nuclei on Atmospheric Radiation *J. Atmos. Sci.* **66**: 41–61

List of Tables

TABLE 1. Model parameterisations investigated. All units are MKS.

Microphysics scheme	$C(D)$	$m(D)$	$v(D)$ (at 1000hPa)	line on Figs. 6 – 9
Wilson and Ballard (1999)	$0.5D$	$0.069D^2$	$25.2D^{0.527}$	Light grey solid
Altered W&B scheme	$0.5D$	$0.0185D^{1.9}$	$25.2D^{0.527}$	Light grey dashed
Hong et al. (2004)	D/π	$(D/11.9)^2$	$1.49 \times 10^4 D^{1.31}$	Black dash-dot
Rutledge and Hobbs (1983):				
cloud ice, $D < 500\mu$m	D/π	$(D/16.3)^2$	0	Black dashed
snow, $D \geq 500\mu$m	D/π	$100\frac{\pi}{6}D^3$	$1.139D^{0.11}$	
Thompson et al. (2008):				
cloud ice, $D < 200\mu$m	$0.5D$	$500\frac{\pi}{6}D^3$	$1847.5D$	Dark grey
snow, $D \geq 200\mu$m	0.3–0.5 $\times D$	$0.069D^2$	$40D^{0.55}\exp(-125D)$	lines & shading

TABLE 2. Fitted parameters controlling the relationship $(C \times f)[\mu\text{m}] = b_1 m[\text{ng}]^{b_2}$. Also shown are parameters for Koenig (1971)'s formula: $\frac{\text{d}m}{\text{d}t}[\text{g/s}] = a_1 m[\text{g}]^{a_2}$ at 1000hPa.

T [°C]	b_1	a_2	a_1 at 1000hPa
-3.7	8.484	0.293	7.95×10^{-8}
-5.3	3.661	0.509	3.95×10^{-6}
-8.6	6.396	0.346	3.14×10^{-7}
-10.6	7.522	0.329	2.81×10^{-7}
-12.2	3.755	0.451	1.82×10^{-6}
-14.4	0.214	0.917	1.59×10^{-3}
-16.5	1.214	0.659	4.32×10^{-5}
-18.2	5.587	0.383	6.29×10^{-7}
-20.1	7.484	0.334	2.89×10^{-7}
-22.0	7.839	0.313	1.83×10^{-7}

List of Figures

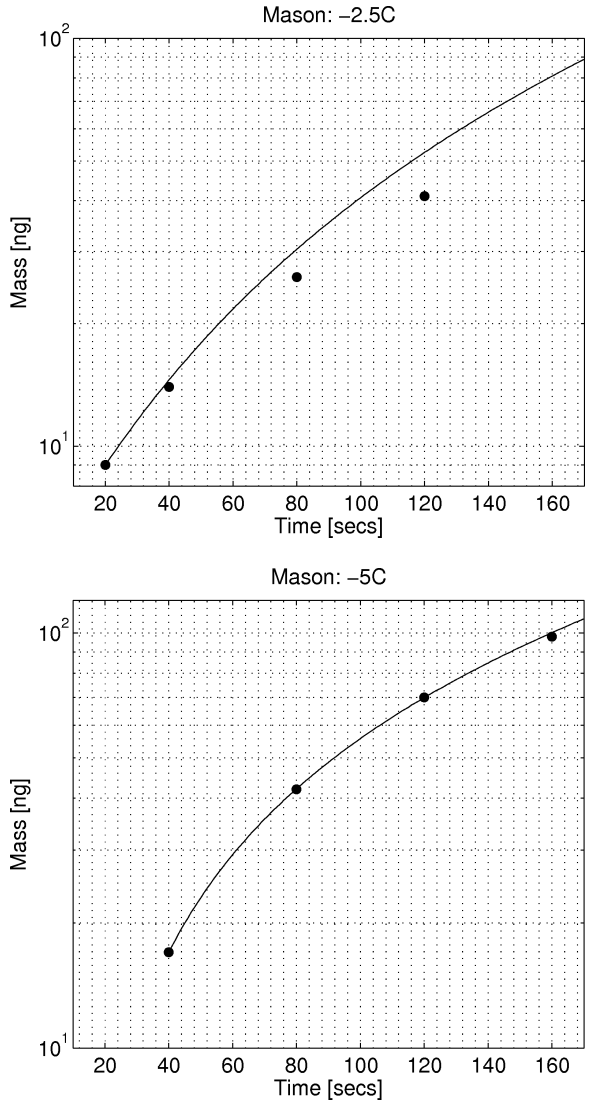

FIG. 1. Comparison with experimental data of Mason (1953). Data points are experimental data, solid curves are predicted $m(t)$ from capacitance theory.

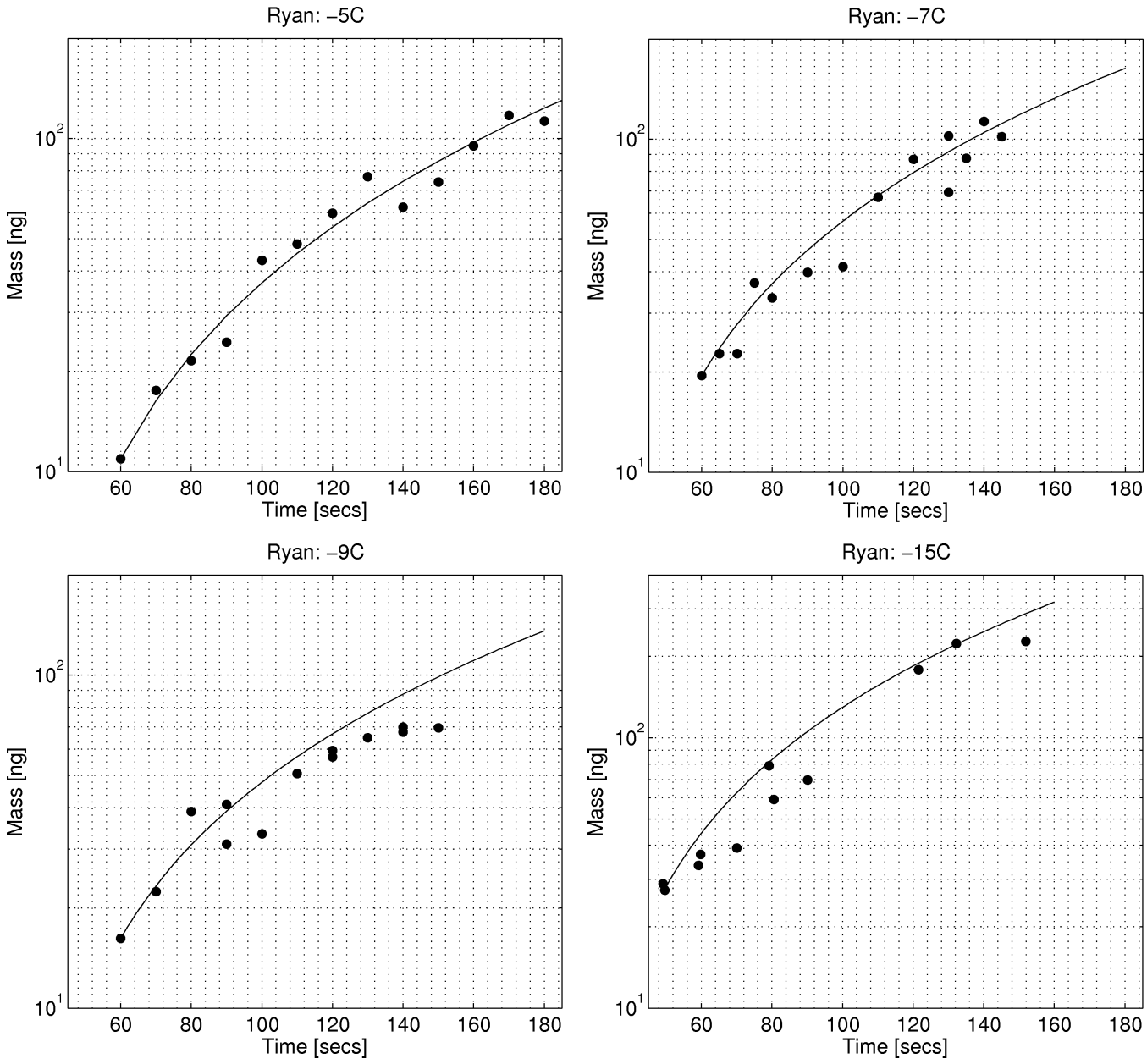

FIG. 2. Comparison with experimental data from Ryan et al. (1974, 1976). Data points are experimental data, solid curves are predicted $m(t)$ from capacitance theory.

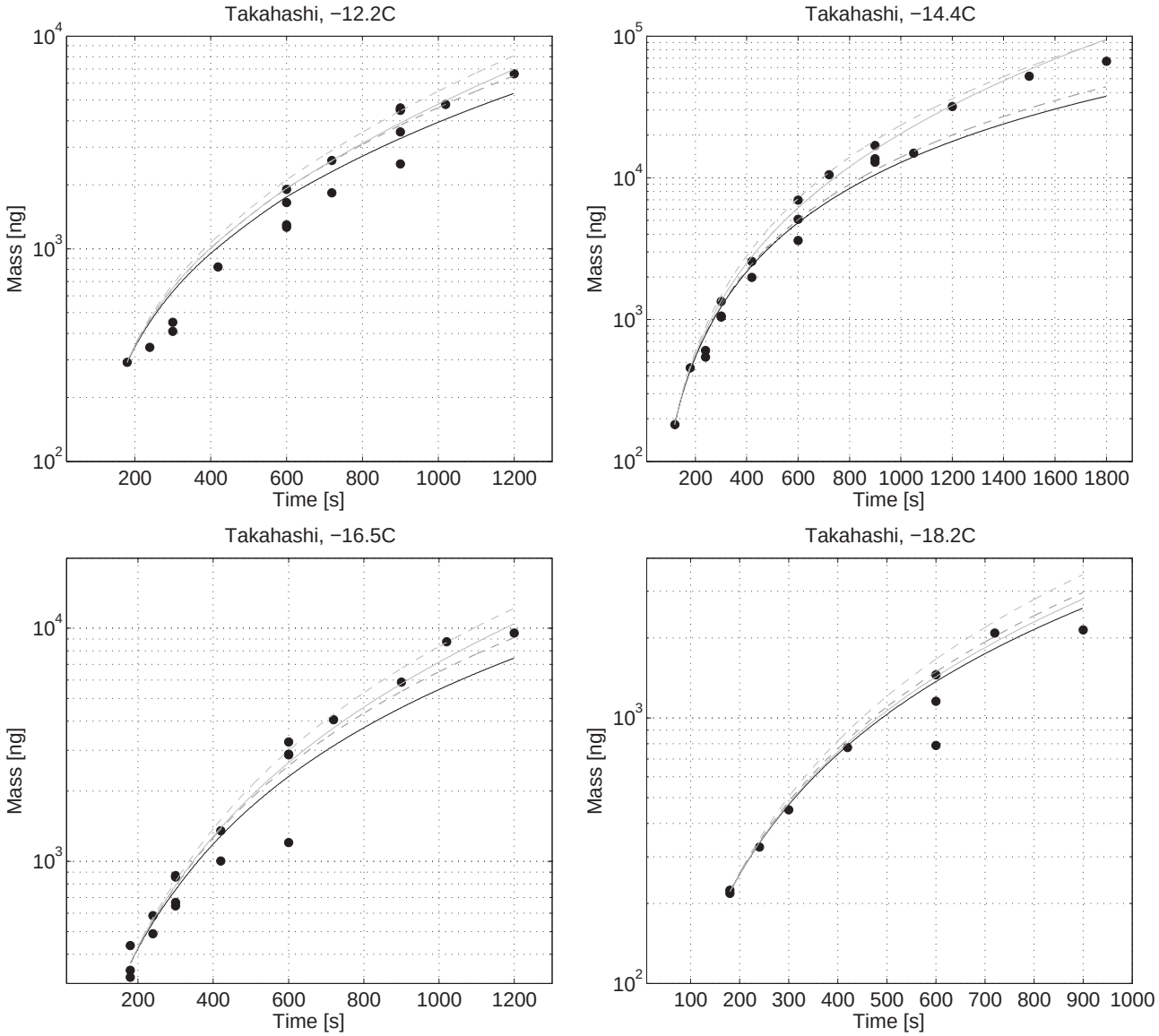

FIG. 3. Crystal mass as a function of time for planar crystals grown by Takahashi et al. (1991) (data points). Black curve is diffusion-limited growth calculated from integrating Eq. (1); dashed dark grey curve includes the HP ventilation factor; dashed light grey curve uses the HPD ventilation factor. The solid grey curve is for the JW ventilation factor.

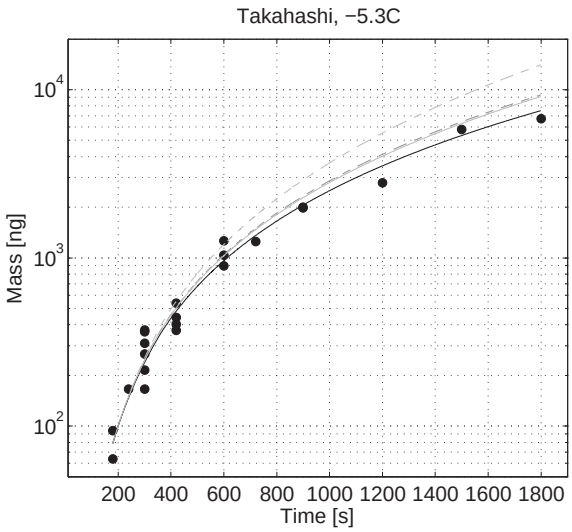

FIG. 4. Crystal mass as a function of time for column and needle crystals grown by Takahashi et al. (1991) (data points). Lines are same as Fig.3.

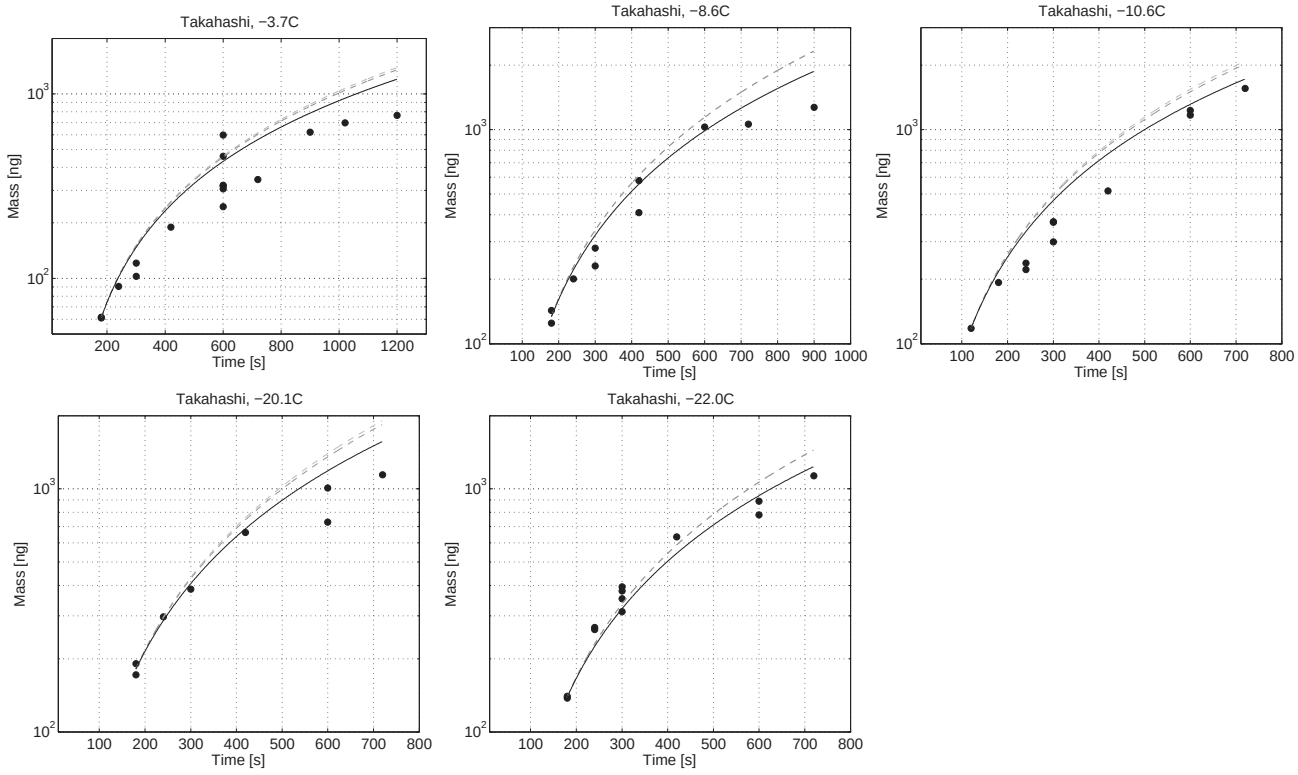

FIG. 5. Crystal mass as a function of time for isometric crystals grown by Takahashi et al. (1991) (data points). Lines are same as Fig.3.

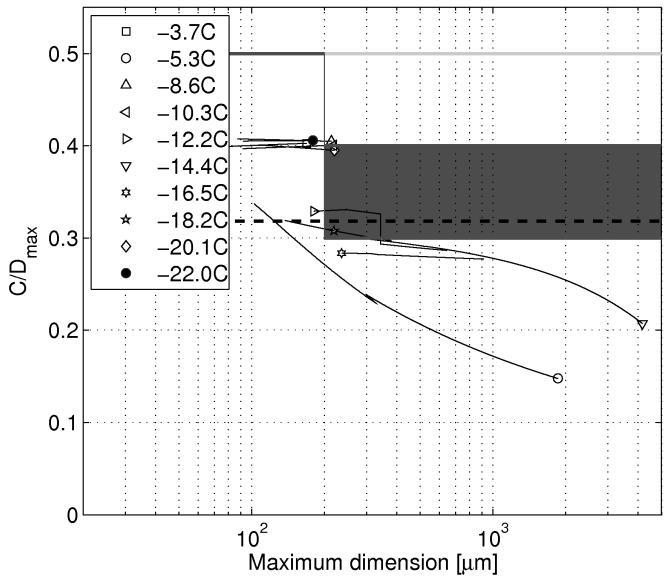

FIG. 6. Relationship between crystal capacitance and maximum dimension, as derived from Takahashi experimental data (thin lines with symbols) along with various model parameterisations (thick lines and shaded area, see table 1).

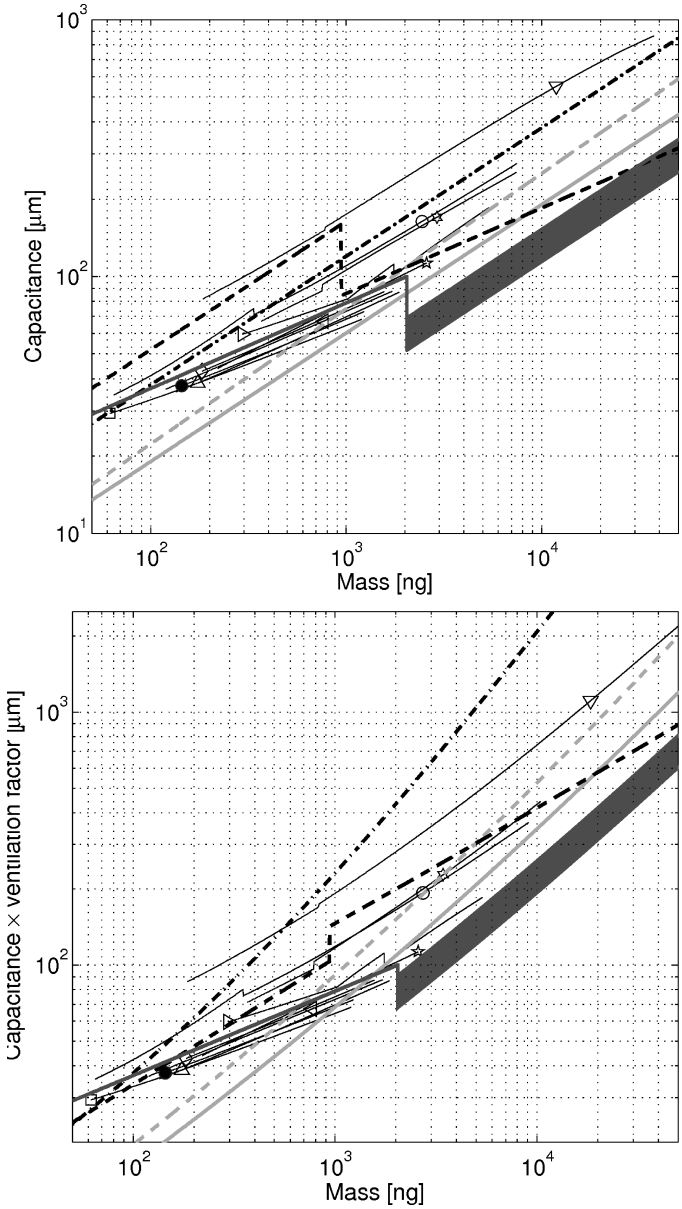

FIG. 7. Upper panel shows relationship between crystal mass and capacitance as derived from experimental data (thin lines with symbols - for key see figure 6) and the relationship implicit in various model schemes (thick lines and shaded area, see table 1). Lower panel shows same, but with ordinate multiplied by ventilation factor f (see text for details). For symbol key, see legend in figure 6.

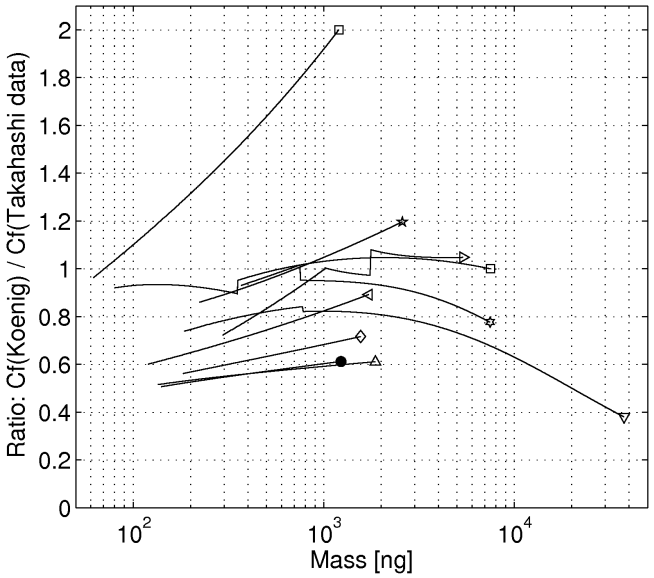

FIG. 8. Ratio of growth rate predicted by Koenig (1971) to that derived from the Takahashi experimental data, as a function of crystal mass. For symbol key, see legend in figure 6.

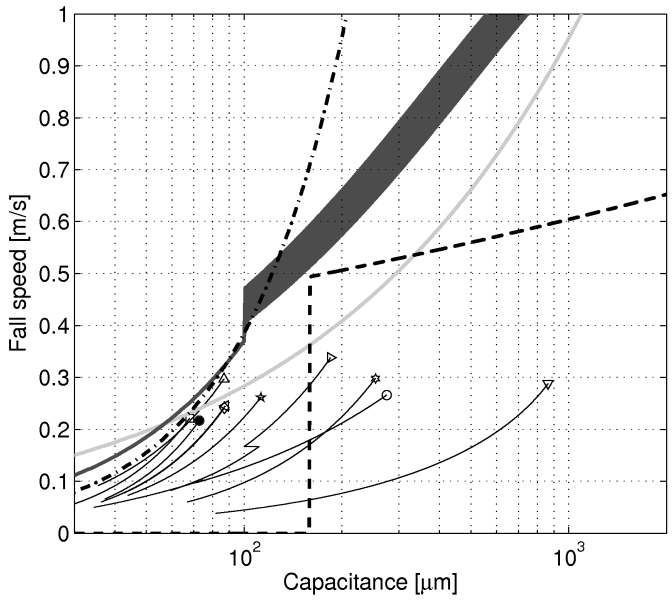

FIG. 9. Relationship between crystal fall speed and capacitance, as derived from Takahashi experimental data (thin lines with symbols) along with various model parameterisations (thick lines and shaded area, see table 1). For symbol key, see legend in figure 6.

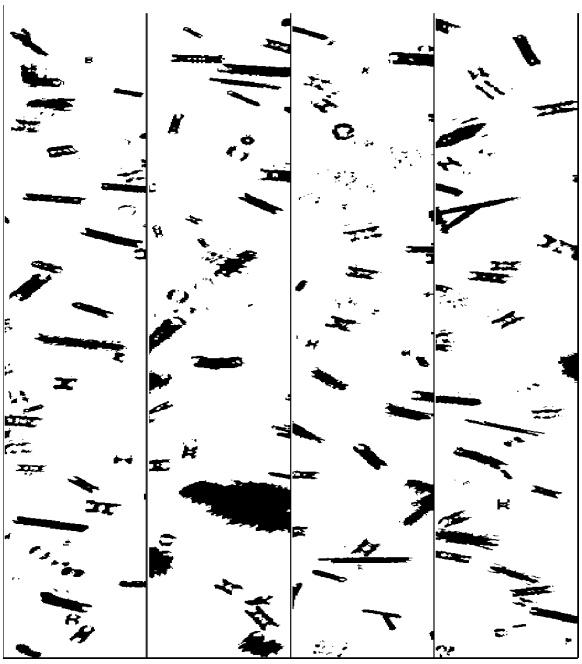

FIG. 10. Pristine vapour-grown needles and sheaths produced via the Hallett-Mossop process in a convective cloud, sampled near the $-5°$C level by Crosier et al. (2011) using a 2DS shadow probe (Lawson et al. 2006). A large rimed crystal is also present in the second strip of images. Image strips are 1.28mm wide, pixels resolution is 10μm.